

NUMERICAL SIMULATION BY A FINITE ELEMENT METHOD  
OF THE SECOND BREAKDOWN OF POWER VERTICAL DMOS TRANSISTORS

H. BELHADDAD<sup>\*\*</sup>, M. LE HELLEY<sup>\*\*</sup>, J.P. CHANTE<sup>\*\*</sup>,  
A. PONCET<sup>†</sup>, G. MERCKEL<sup>†</sup>

<sup>\*\*</sup>LEAME, ERA CNRS n°661 - E.C.L. - BP 163 - 69131 ECULLY Cedex (F)  
<sup>†</sup>CNET CNS - BP 42 - 38240 MEYLAN (F)

ABSTRACT

The two-dimensional simulation of the breakdown of power vertical DMOS transistor is presented. The finite-element method is used to solve the full set of the equations of the physics of semiconductor. It is shown that second breakdown can be initiated by the body effect in the MOS transistor rather than by the turn-on of the parasitic bipolar device. The factor is the resistance of the p-layer in a n channel MOS transistor.

I. INTRODUCTION

The performances of vertical power MOSFET's can be limited in high-voltage, high-current range by the phenomenon of second breakdown as depicted in Fig.1. The explanation for

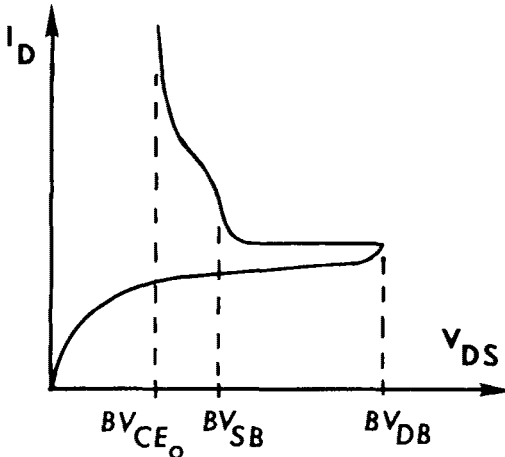


Fig.1 : Second breakdown in n-channel power vertical MOS transistor.

this phenomenon has been given in Ref.[1] as for the case of lateral power DMOS [2] and as it has been done for classical structures [3],[4],[5],[6]. It involves the turn-on of the parasitic bipolar transistor, see Fig.2, when the drain voltage is increased.

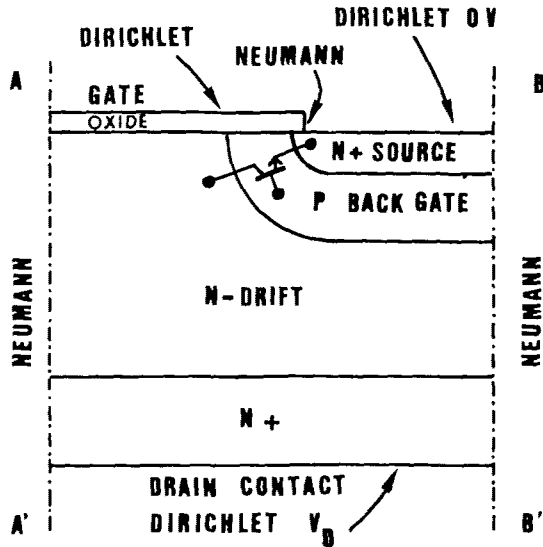


Fig.2 : Cross-section of vertical DMOS transistor

Quantitative results based on an one-dimensional analysis are given in Ref.[7] for the second breakdown of vertical power MOSFET's. The purpose of this paper is to present results obtained by numerical two-dimensional simulations.

## II. EQUATIONS

Because the phenomenon of second breakdown is induced by avalanche multiplication the full set of complete equations of the physics of semiconductor must be solved. These equations are [8].

- 1) POISSON's equation in semiconductor

$$\Delta\psi = -\frac{q}{\epsilon} (N_D^+ - N_A^- + p-n)$$

or LAPLACE's equation in insulator which is assumed free of charge

$$\Delta\psi = 0$$

- 2) Current equations

$$j_n = -q \mu_n n \nabla\psi_n$$

$$j_p = -q \mu_p p \nabla\psi_p$$

3) Carrier density equations as given by BOLTZMANN's statistics

$$n = n_i \exp \frac{\psi - \psi_n}{V_T}$$

$$p = n_i \exp \frac{\psi_p - \psi}{V_T}$$

4) Continuity equations

$$\nabla \cdot j_n = q (G_n - R_n)$$

$$\nabla \cdot j_p = q (G_p - R_p)$$

5) Generation-recombination equation following SCHOCKLEY-READ-HALL model and including avalanche generation

$$G_n - R_n = -(G_p - R_p) = \frac{p_n - n_i^2}{\tau_{n0}(p+n_i) + \tau_{p0}(n+n_i)} - \alpha_n |J_n| - \alpha_p |J_p|$$

The ionization coefficients are given by

$$\alpha_{n,p} = A_{n,p} \exp - \frac{b_{n,p}}{|E|}$$

6) Electric-field-potential relation

$$E = - \nabla \psi$$

### III. NUMERICAL METHOD

The finite-element code DELTA of CNET<sup>(\*)</sup> is used to solve iteratively the set of previously defined equations where potential  $\psi$  and quasi-FERMI levels  $\psi_n$  and  $\psi_p$  are the three unknowns.

GUMMEL's algorithm [9] is employed to calculate  $\psi$  from the known values of  $\psi_n$  and  $\psi_p$  then to use the newly calculated values of  $\psi$  to update quasi-FERMI levels  $\psi_n$  and  $\psi_p$  until the convergence is obtained. POISSON's equation and continuity equations are solved by a NEWTON's and an one-point iterative methods respectively. Linear triangular elements are employed to discretize the device.

### IV. DEVICE AND BOUNDARY CONDITIONS

The studied structure which is the active part of a vertical DMOS transistor is shown schematically in Fig.2 ; it is in fact one-half of an elementary cell where AA' is the axis of symmetry.

The boundary conditions for the potential are given in Fig.2 ; for the carrier concentrations we assume equilibrium values at the contacts and NEUMANN boundary conditions on AA' and BB'.

(\*) Centre National d'Etudes des Télécommunications (France)

A finite-element model of all the device is shown in Fig.3.a ; a zoomed representation around the N+P and PN<sup>-</sup> junctions is depicted in Fig.3.b. The geometrical dimensions of a studied device are indicated in these schemas.

V. RESULTS AND DISCUSSION

Potential distributions for different bias conditions are shown in Fig.4 within all the structure and within the zoomed area in Fig.5.

The forward bias of the source-backgate junction when the drain voltage is increased is proved by the increasing from its equilibrium value of the potential at points within the neutral area of the backgate region, see Fig.5. Also the increasing of the quasi-Fermi potential  $\psi_p$  is observed. These facts do not appear if the multiplication terms are deleted in generation-recombination equation.

As shown in Fig.6, the emitter-base junction of the parasitic bipolar transistor is a little forward-biased whereas the drain voltage is increased to attain the high multiplication range. Nevertheless, due to the body-effect in the MOS

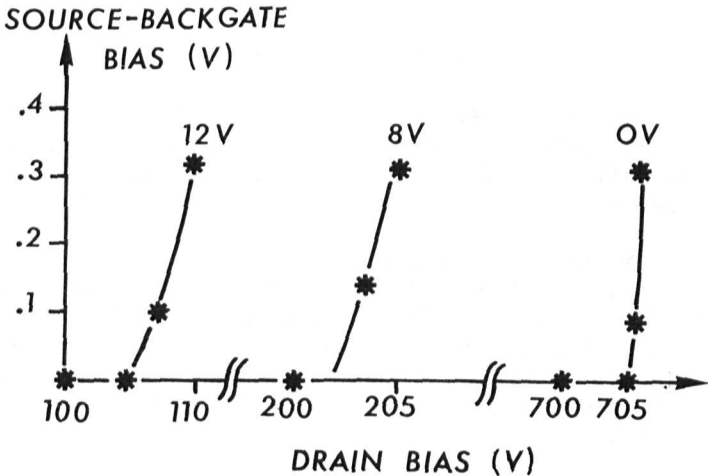


Fig.6 : Source-back gate forward bias versus drain-source voltage with gate voltage as a parameter

transistor rather than the bipolar turn-on a negative resistance effect can occur. First the breakdown of the drain-backgate junction is for  $BV_{DB}$  which depends on the potential distribution in its depleted area. This potential distribution is determined by the drain and gate voltages and by the space charge which is given by ionized atoms plus the charges injected by the channel. The values of  $BV_{DB}$  obtained by simulation are given in Fig.7.

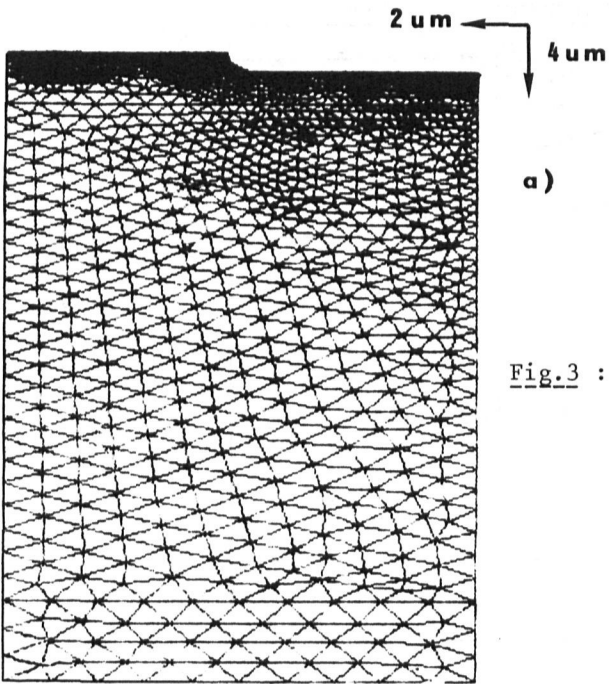
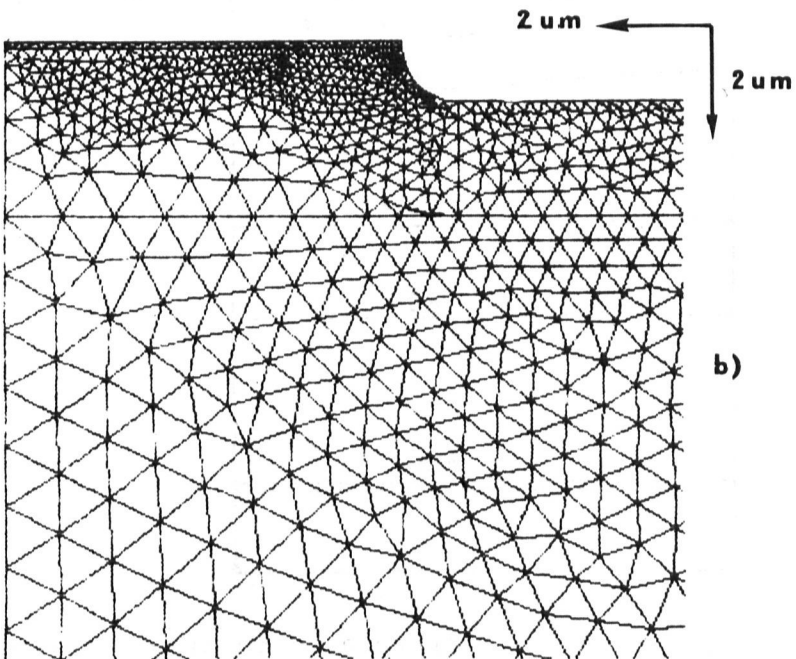
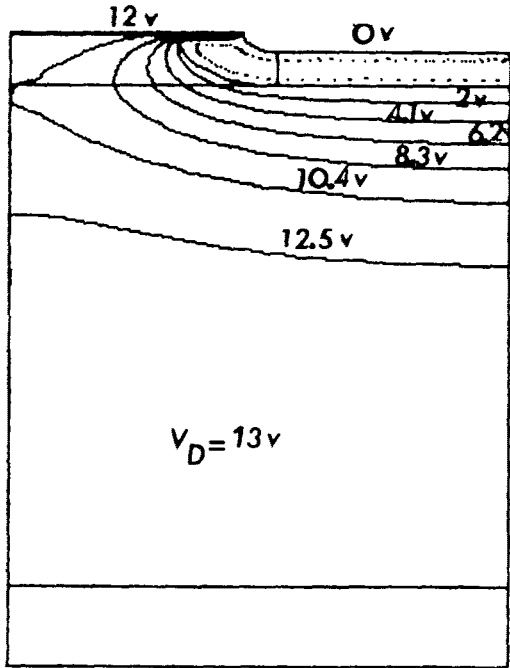
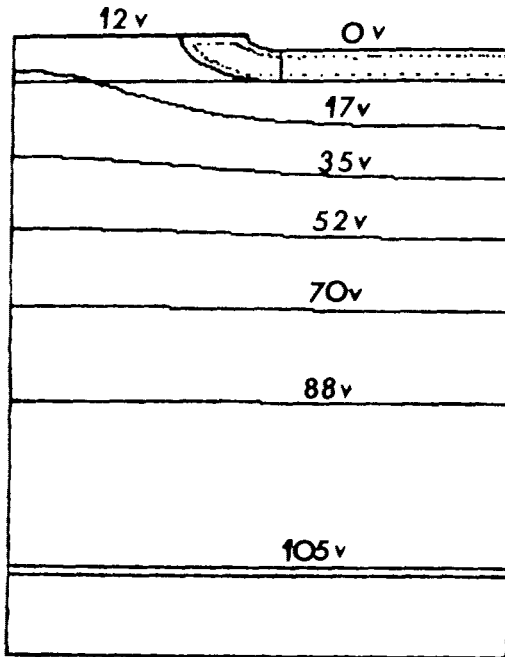


Fig.3 : Finite-element model





(a)



(b)

Fig.4 : Potential distribution within all the structure  
 a)  $V_D = 13V$  ; b)  $V_D = 105V$

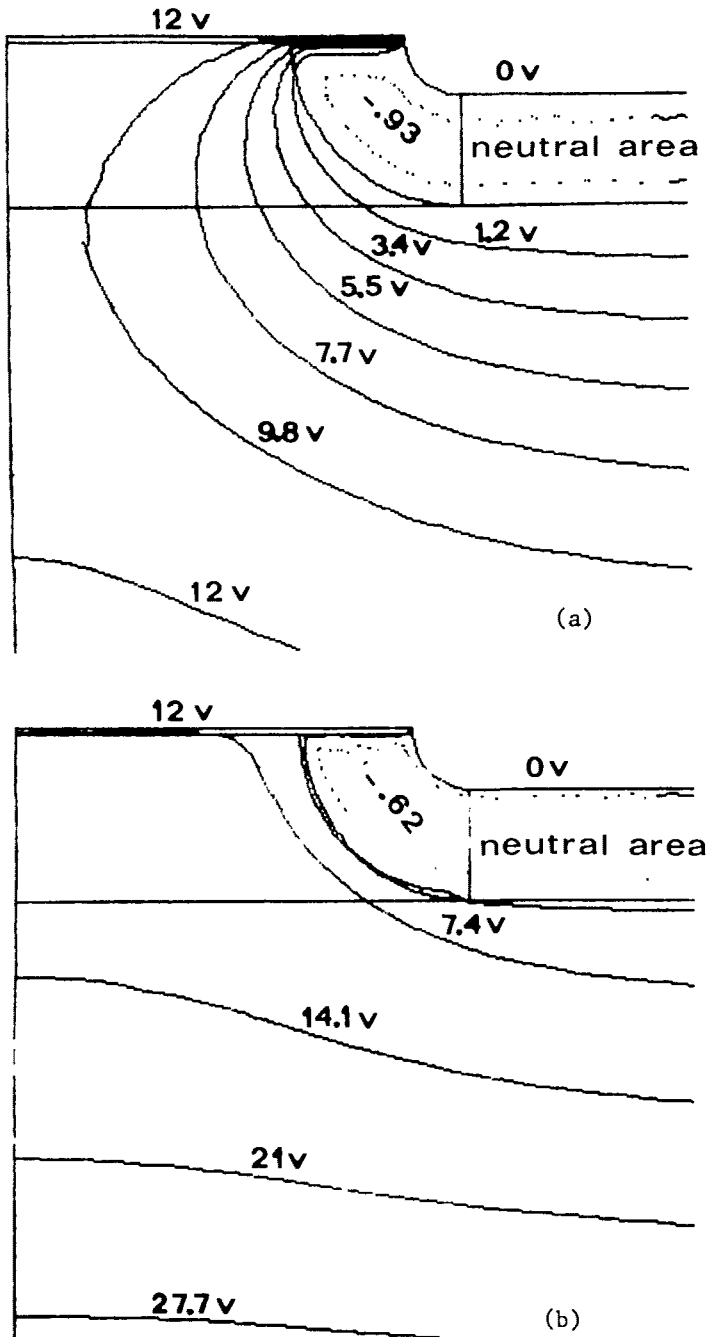
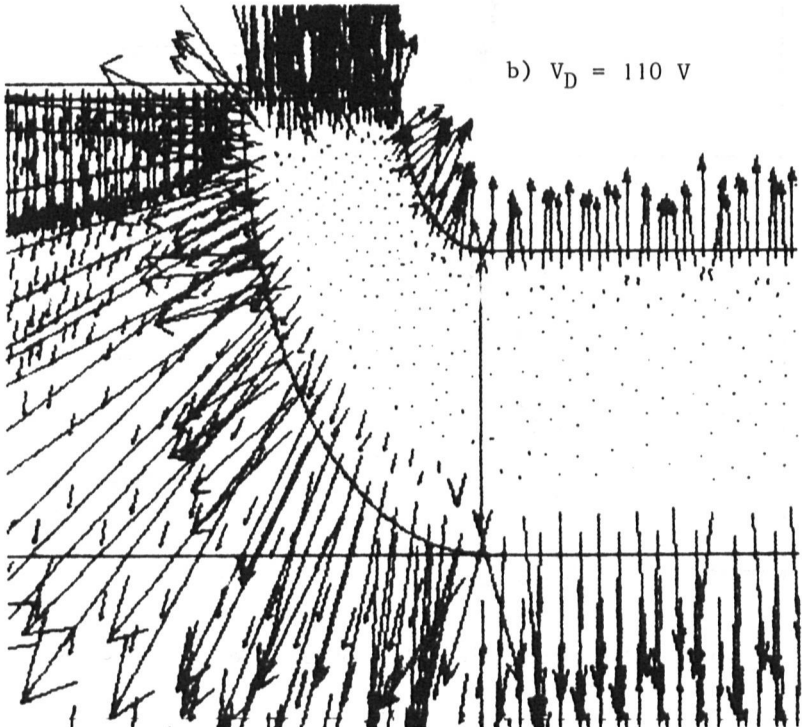
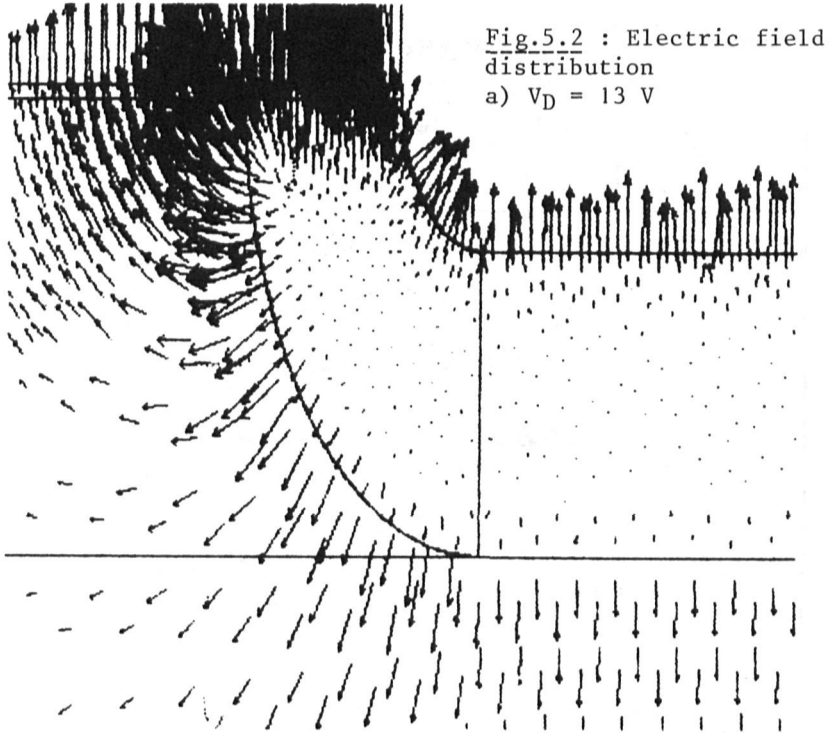


Fig.5.1 : Potential distribution in the zoomed area  
 a)  $V_D = 13 \text{ V}$  ; b)  $V_D = 110 \text{ V}$





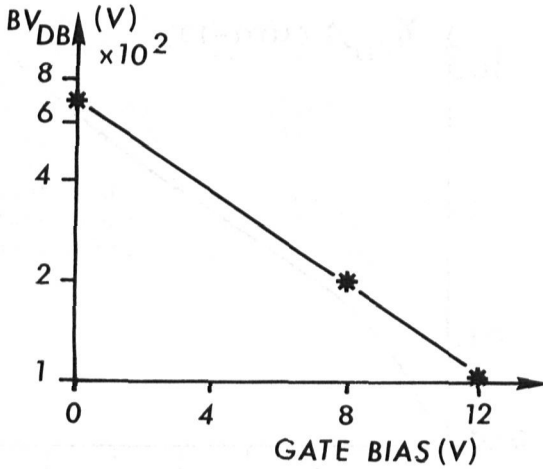


Fig. 7 : Breakdown voltage of back-gate drain junction versus gate bias without substrate effect

The hole current given by the avalanche multiplication flows in the base of the bipolar transistor. At the beginning this current yields a little forward bias but which can be sufficient to induce snap-back due to the body effect in the MOS structure.

The breakdown voltage with snap-back which is given [7] by

$$BV_{SB} = BV_{DB} \left( \frac{1}{1 + \gamma r_b} \right)^{1/n}$$

depends on the body factor  $\gamma$  and the base resistance  $r_b$ . A simple expression for the body factor can be defined.

$$\gamma = Z v_s (2 \epsilon q N_A)^{1/2} \left( \frac{\sqrt{2\phi_p} - \sqrt{2\phi_p - V_B}}{V_{bi} - V_B} \right)$$

Once all the physical parameters of the MOS transistor are designed, the value of  $\gamma r_b$  is determined by the length  $\ell$  of the base resistance. This length depends on the location of the shorts between the source and the back-gate layers. Values of  $\gamma r_b / \ell$  for a typical case are shown in Fig. 8.

Then the turn-on of the bipolar transistor arises when the level of the hole current is sufficient to forward-bias the emitter-base junction. A second snap-back

$$BV_{CEo} = \frac{BV_{DB}}{(\beta)^{1/n}}$$

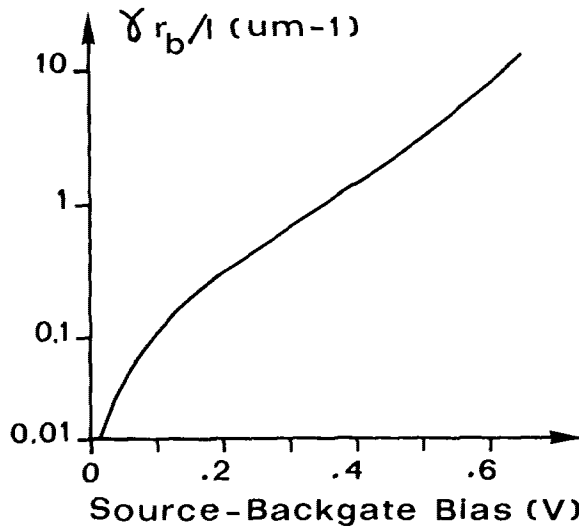


Fig.8 : Body factor versus source-backgate forward bias  
 $L = 2 \mu\text{m}$  ;  $e = 2 \mu\text{m}$  ;  $N_A = 5 \times 10^{16} / \text{cm}^3$

can be found as depicted in Fig.1. Of course, if the value of the base resistance is small only this last snap-back effect exists.

#### REFERENCES

- [1] COEN, R.W., TSANG, D.W., LISIAK, K.P.  
 A high-performance planar power MOSFET  
 IEEE Trans.Electron.Dev., ED-27, 340 (1980)
- [2] YOSHIDA, I., OKABE, T., KATSUEDA, M., OCHI, S., NAGATA, M.  
 Thermal stability and secondary breakdown in planar power MOSFET's  
 IEEE Trans.Electron.Dev., ED-27, 395 (1980)
- [3] KENNEDY, D.P. and PHILLIPS Jr, A.  
 Source-drain breakdown in an insulated gate-field-effect transistor  
 Proc.Int.Electron. Devices Meet., 160 (1973)
- [4] MASUDA, H., NAKAI, M., KUBO, M.  
 Characteristics and limitation of scaled-down MOSFET's due to two-dimensional field effect  
 IEEE Trans.Electron.Dev., ED-26, 980 (1979)
- [5] TOYABE, T., YAMAGUCHI, K., ASAI, S., MOCK, M.S.  
 A numerical model of avalanche breakdown in MOSFET's  
 IEEE Trans.Electron.Dev., ED-25, 825 (1978)
- [6] TOYABE, T. and ASAI, S.  
 Analytical models of threshold voltage and breakdown voltage of short-channel MOSFET's derived from two-dimensional analysis  
 IEEE Trans.Electron.Dev., ED-26, 453 (1979)

- [7] HU, C. and CHI, M.H.  
Second breakdown of vertical power MOSFET's  
IEEE Trans.Electron.Dev., ED-29, 1287 (1982)
- [8] SZE, S.M.  
Physics of semiconductor devices  
2nd Edition, John Wiley (1981)
- [9] GUMMEL H.K.  
A self-consistent iterative scheme of one-dimensional  
steady state transistor calculations  
IEEE Trans.Electron.Dev., 11, n°10, 455 (1964)